Defence Technology 13 (2017) 111–117

Contents lists available at ScienceDirect

Defence Technology

journal homepage: www.elsevier.com/locate/dt

Optimizing the micro-arc oxidation (MAO) parameters to attain coatings with minimum porosity and maximum hardness on the friction stir welded AA6061 aluminium alloy welds

R. Kamal Jayaraj [a], S. Malarvizhi [b], V. Balasubramanian [b, *]

[a] Centre for Materials Joining and Research (CEMAJOR), Department of Manufacturing Engineering, Annamalai University, Annamalai Nagar, 608 002, Tamil Nadu, India
[b] Centre for Materials Joining and Research (CEMAJOR), Department of Manufacturing Engineering, Annamalai University, Annamalai Nagar, 608 002, Tamil Nadu, India

ARTICLE INFO

Article history:
Received 15 March 2017
Received in revised form
17 March 2017
Accepted 21 March 2017
Available online 23 March 2017

Keywords:
Micro-arc oxidation
Aluminium alloy
Friction stir weld
Response surface methodology

ABSTRACT

Micro-arc oxidation (MAO) technique is capable of producing dense oxide films on the aluminium alloy surface. This oxide film protects the aluminium alloy from the corrosion attack for longer duration. Empirical relationships were derived to evaluate the MAO coating properties (porosity and hardness) by incorporating very important MAO parameters (current density, inter-electrode distance and oxidation time). MAO parameters were also optimized to achieve coatings with minimum porosity and maximum hardness. Further, the effect of MAO parameters on coating characteristics was analysed. From the results, it is found that the current density has greater influence on the responses than the other two parameters.

1. Introduction

Aluminium and its alloys are extensively joined by the friction stir welding (FSW) process due to the many advantages [1]. The major problems like porosity, hot crack, etc., occurred in fusion welding techniques are completely eliminated by the FSW process due to low heat input and solid state joining of aluminium alloys [2]. The FSW joint consists of four different zones, namely unaffected parent metal, heat affected zone (HAZ), thermo-mechanically affected zone (TMAZ) and stir zone (SZ). Of these four regions, the stir zone consists of finer grains compared to the other zones [3,4].

Number of corrosion studies were carried out on aluminium alloys and its welds [5–8]. The effects of chloride ion concentration and pH level of environment on pitting corrosion of aluminium alloys were studied using potentiodynamic anodic polarization test [9]. It is reported by many researchers that the corrosion behaviour of aluminium alloy was dependent on chloride concentration and pH level of the solution. It is also reported that AA6061 aluminium alloy corroded caused by chemical dissolution of alkaline solutions by the presence of OH^- and at a comparatively low amount in acidic solution. Few studies were carried out to compare the corrosion behaviour of the weld metal with parent metal. Farhad et al. investigated the corrosion behaviour of AA6061 aluminium alloy joint produced by the FSW process [10]. In this the SZ of the FSW joint experienced more corrosion attacks than the parent metal. Also, few researchers reported that the corrosion behaviour of the FSW joint depends on the FSW parameters used to weld the joint [11,12]. It is essential to enhance the corrosion resistance of FSW weldment to avoid corrosion failure of the joint.

Many surface treatment techniques are used to modify the surface of the aluminium alloys [13,14]. Thermal spraying methods such as high velocity oxy-fuel spraying, plasma spraying, detonation spraying are extensively used in now-a-days, but these coatings are capable to enhance the corrosion resistance to some extent due to the mechanical bonding of the coating with substrate. However, micro-arc oxidation (MAO) technique provides a better bonding (metallurgical) between the component and coating. MAO coating improves the corrosion and wear resistance of the aluminium alloys compared to many other coatings [15]. In this

* Corresponding author.
E-mail addresses: jayaraj_kamal@yahoo.co.in (R. Kamal Jayaraj), jeejoo@rediffmail.com (S. Malarvizhi), visvabalu@yahoo.com (V. Balasubramanian).
Peer review under responsibility of China Ordnance Society

http://dx.doi.org/10.1016/j.dt.2017.03.003

investigation, an attempt has been made to identify the optimum MAO parameters to attain protective coatings with minimum porosity and maximum hardness on the stir zone of FSW joints of AA6061 aluminium alloy.

1.1. Experimental work

The parent metal used in this study was AA6061 aluminium alloy with a thickness of 6 mm. The alloy composed of 1% Mg, 0.6% Si, 0.2% Cr, 0.25% Cu and remaining Al in weight percentage. The joints were fabricated with the taper cylindrical tool using optimised welding parameters. The dimensions of tool and optimised FSW parameters are listed in Table 1.

The major influencing MAO parameters were identified and selected from the literatures [16–18]. Among the several independently controllable primary and secondary MAO parameters, which affects the coating property of the aluminium alloy, the parameters considered in this investigation are current density (I), inter-electrode distance (D) and oxidation time (T).

Many preliminary trial experiments were conducted using the specimen extracted from SZ of FSW joints (50 mm × 20 mm) to identify the working limits of MAO parameters. Various combinations of MAO parameters were used during the trial experiments and the following inferences were made:

(i) If the current density was <0.04 A/cm^2, the micro-arc on the surface of the aluminium alloy did not formed due to insufficient of current.
(ii) If the current density was >0.20 A/cm^2, the surface of the coated material was composed of loose and pores oxide film due to excess current applied.
(iii) There is a constraint in the electrolytic bath so the minimum and maximum inter-electrode distance was kept 4 and 8 cm respectively.
(iv) If the oxidation time was <10 min, the coating was formed with a very lower hardness.
(v) If the oxidation time was >50 min, the micro-arc was extinguished.

Specially designed electrical controller MAO coating unit of 30 kVA was used in the present study (Fig. 1(a)). An alkali solution with a mixture of potassium hydroxide and sodium meta silicate was employed as electrolyte in this present work. The temperature of the electrolyte is maintained at 20–30 °C during the process with a help of the chiller. The electrolyte gets cooled in chiller and it circulated throughout the process. Substrate (specimen) was connected to an AC power source (high-voltage) with a constant current density all over the coating process. The substrate immersed fully in the electrolyte bath in a non-conductive container (Fig. 1(b)). The range of factors considered is given in Table 2 and the 20 sets of experimental conditions employed are given in Table 3. The photographs of uncoated and coated specimens are displayed in Fig. 1(c–d) respectively. The morphology (top surface and cross-section) of the coatings were analysed using secondary electron microscopy (JEOL-JSM-5610LV) and then the percentage of porosity was measured with an image analysis software. X-Ray diffraction (XRD) analysis was carried out using an X-ray diffractometer (special attachment no. HTK 1200, Anton Paar, Austria, Europe) of XPert, to find out the phases present in the MAO coatings.

1.2. Developing empirical relationships

The coating porosity and coating hardness (Y) are the functions of MAO parameters such as current density (I), inter-electrode distance (D) and oxidation time (T), and it is given by following expression.

$$Y = f\{I, D, T\} \tag{1}$$

Second-order polynomial (regression) equation used to represent the response surface Y is given by

$$Y = b_0 + \Sigma b_i x_i + \Sigma b_{ii} x_i^2 + \Sigma b_{ij} x_i x_j \tag{2}$$

The response (Y) can be expressed in the form of MAO parameters as given below

$$Y = b_0 + b_1(I) + b_2(D) + b_3(T) + b_{12}(ID) + b_{13}(DT) + b_{23}(IT) + b_{11}\left(I^2\right) + b_{22}\left(D^2\right) + b_{33}\left(T^2\right) \tag{3}$$

Where, the average response is denoted by b_0 and b_1,b_2,b_3, are linear responding terms; b_{12},b_{13},b_{23} are the response of interaction terms; b_{11},b_{22},b_{33} are the responses of squared terms. Analysis of Variance (ANOVA) test was conducted for both the responses and the results are shown in Tables 4 and 5. From the results, it is understood that the F-value for the developed porosity and hardness models is 324.82 and 86.80 respectively and suggest that the models are significant. For these models, there is a 0.01% chance that a "Model F-Value" this large could occur due to noise. Values of "$Prob > F$" less than 0.0500 indicates the model terms are significant. In hardness I, T, DT, I^2 and T^2 are significant model terms and in porosity I, D, T, ID, IT, DT, I^2, C^2 and T^2 are the significant model terms. The values of "$Prob > F$" greater than 0.1000 indicates that the model terms are not significant.

For the porosity and hardness the "Lack of Fit F-value" of 3.39 and 3.20 respectively, indicates the "Lack of Fit" is not significant relative to a pure error. There is a 10.34% and 11.38% chance that a "Lack of Fit F-value" this large could happen due to noise for porosity and hardness respectively. Non significant lack of fit is good for both the model. For the porosity "Pred R-Squared" of 0.9772 is in reasonable conformity with the "Adj R-Squared" of 0.9935 and for the hardness the "Pred R-Squared" of 0.9207 is in reasonable conformity with the "Adj R-Squared" of 0.9760. "Adeq Precision" calculates the signal to noise ratio and the ratio larger than 4 is desirable. The ratio for porosity of 57.790 and hardness of 33.311 indicates an adequate signal.

The empirical relationships were developed using only with the significant co-efficients and the constructed final empirical relationships were given below

Table 1
FSW parameters and tool dimensions.

Tool rotational speed/rpm	Tool travel speed/(mm·min^{-1})	Axial force/kN	Tool shoulder diameter/mm	Tool pin diameter/mm	Tool pin length/mm	Tool pin profile
1000	30	5.5	18	5–6	5.7	Taper cylindrical

Fig. 1. Experimental details.

Table 2
Important MAO parameters and their levels.

S.No.	Factor	Notation	Levels				
			−1.68	−1	0	+1	+1.68
1	Current density	$I/(A\cdot cm^{-2})$	0.04	0.07	0.12	0.17	0.20
2	Inter-electrode distance	D/cm	4	4.81	6	7.19	8
3	Oxidation time	T/min	10	18.11	30	41.89	50

$$Coatingporosity = \{2.04 + 1.10I - 0.40D + 0.60T + 0.38ID - 0.42IT + 0.46DT + 3.23I^2 + 0.27D^2 + 1.82T^2\}vol\% \quad (4)$$

To confirm the constructed empirical relationships, three tests were conducted with the MAO parameters selected randomly from the feasible working limits (Table 2). The actual response was calculated as the average of three measured results. From the validation results (Table 6), it is evident that the constructed empirical relationships were relatively accurate as the variation in prediction is ±5%.

$$Coating\ hardness = \{1334.69 - 77.98I + 11.29D - 53.37T - 18.25ID + 11.75IT - 41.75DT - 203.79I^2 + 6.22D^2 - 62.72T^2\}HV \quad (5)$$

Table 3
Design matrix and experimental results.

Experiment number	Factors			Responses	
	I	*D*	*T*	Coating porosity/(vol%)	Coating hardness/HV
1	0.07	4.81	18.11	6.47	1180
2	0.17	4.81	18.11	8.53	986
3	0.07	7.19	18.11	3.62	1312
4	0.17	7.19	18.11	7.88	1088
5	0.07	4.81	41.89	7.46	1096
6	0.17	4.81	41.89	8.52	992
7	0.07	7.19	41.89	7.14	1104
8	0.17	7.19	41.89	9.03	884
9	0.04	6.00	30.00	9.52	846
10	0.20	6.00	30.00	12.93	654
11	0.12	4.00	30.00	3.48	1338
12	0.12	8.00	30.00	2.17	1350
13	0.12	6.00	10.00	6.48	1220
14	0.12	6.00	50.00	7.95	1078
15	0.12	6.00	30.00	1.92	1354
16	0.12	6.00	30.00	2.3	1305
17	0.12	6.00	30.00	1.92	1352
18	0.12	6.00	30.00	2.24	1310
19	0.12	6.00	30.00	1.92	1346
20	0.12	6.00	30.00	1.92	1344

Table 4
ANOVA test results for coating porosity.

Source	Sum of squares	*df*	Mean square	*F* value	*p*-value Prob > *F*	significant
Model	211.76	9	23.53	324.82	<0.0001	
I	16.49	1	16.49	227.59	<0.0001	
D	2.23	1	2.23	30.72	0.0002	
T	4.83	1	4.83	66.69	<0.0001	
ID	1.15	1	1.15	15.84	0.0026	
IT	1.42	1	1.42	19.60	0.0013	
DT	1.70	1	1.70	23.50	0.0007	
I^2	150.83	1	150.83	2082.23	<0.0001	
D^2	1.01	1	1.01	14.00	0.0038	
T^2	47.60	1	47.60	657.12	<0.0001	
Residual	0.72	10	0.072			
Lack of Fit	0.56	5	0.11	3.39	0.1034	not significant
Pure Error	0.17	5	0.033			
Cor Total	212.49	19				

Table 5
ANOVA test results for coating hardness.

Source	Sum of squares	*df*	Mean square	*F* value	*p*-value *Prob* > *F*	significant
Model	7.796E+005	9	86 627.39	86.80	<0.0001	
I	83 036.77	1	83 036.77	83.20	<0.0001	
D	1740.66	1	1740.66	1.74	0.2160	
T	38 894.07	1	38 894.07	38.97	<0.0001	
ID	2664.50	1	2664.50	2.67	0.1333	
IT	1104.50	1	1104.50	1.11	0.3176	
DT	13 944.50	1	13 944.50	13.97	0.0039	
I^2	5.985E+005	1	5.985E+005	599.69	<0.0001	
D^2	557.25	1	557.25	0.56	0.4721	
T^2	56 699.43	1	56 699.43	56.81	<0.0001	
Residual	9980.45	10	998.04			
Lack of Fit	7603.61	5	1520.72	3.20	0.1138	not significant
Pure Error	2376.83	5	475.37			
Cor Total	7.896E+005	19				

1.3. Relationship between coating porosity and coating hardness

The experimentally measured porosity and hardness values of the coatings (presented in Table 3) are plotted in a linear graph as shown in Fig. 2. All the points, fitted and connected by a best fit and the equation for the best fit line is given by

$$\text{Coating Hardness (HV)} = 1489 - 58.68(\text{Porosity, Vol.\%}) \quad (6)$$

The slope of the best fit line (−58.68) is negative and it suggests that the porosity is having the opposite effect with hardness. The co-efficient of determination, R^2 is found to be 92.6% of the above equation. The coefficient of determination, R^2 will provide

Table 6
Validation test results.

Si.No	I/(A·cm^{-2})	D/cm	T/min	Variation/%	
				Coating porosity/(vol%)	Coating hardness/HV
1	0.05	7	25	−1.75	+0.89
2	1.2	5	35	+1.08	+1.12
3	1.8	6	45	−1.26	−1.24

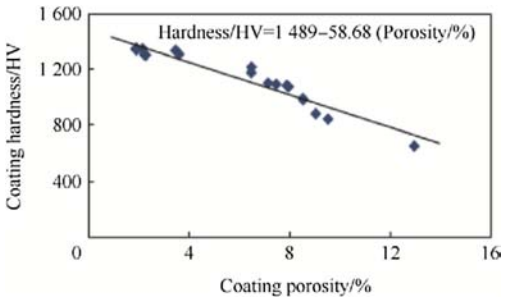

Fig. 2. Relationship between porosity and hardness.

information about the goodness of fit of the derived regression equation. The above derived equation can be utilized to determine the mean value of coating hardness for a given level of coating porosity.

1.4. Optimizing MAO parameters

The response surface methodology (RSM) was employed to optimize the MAO parameters in this work. In the response plot the lowest point shows the minimum achievable responses (coating porosity) and the peak point shows the maximum achievable values (coating hardness). The aim of the optimization involves achieving maximum hardness with a minimum percentage of porosity. By analyzing the contour plots and response surface plots as shown in Figs. 3 and 4, the minimum porosity recorded is found to be 1.76 vol% and the maximum achievable coating hardness is 1360 HV. The corresponding MAO parameters that yielded the minimum porosity with maximum hardness are current density of 0.11 A/cm^2, inter-electrode distance of 6.33 cm and oxidation time of 26.61 min.

1.5. Characteristics of MAO coating

Top surface area and cross-sectional view of the MAO coated stir zone of FSW joint are characterised by scanning electron

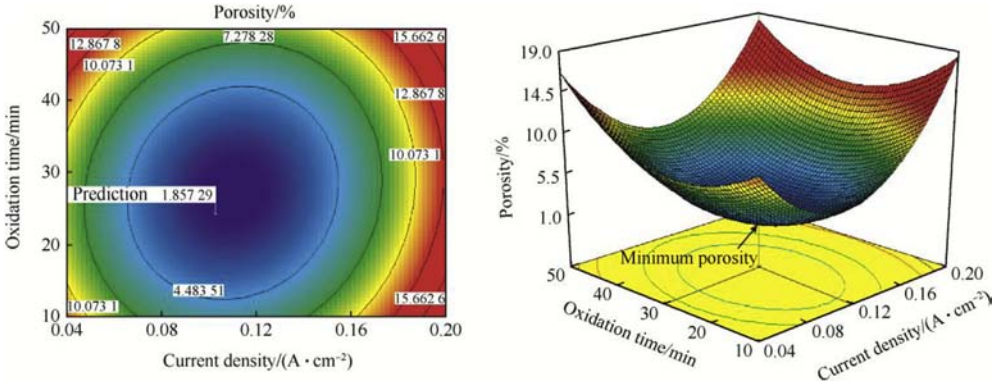

Fig. 3. Response and contour graphs for porosity of MAO coat between current density and oxidation time.

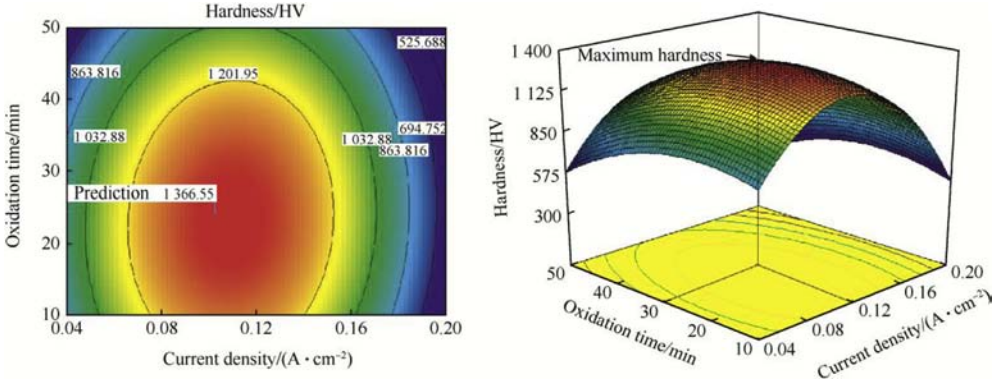

Fig. 4. Response and contour graphs for coating hardness of MAO coat between current density and oxidation time.

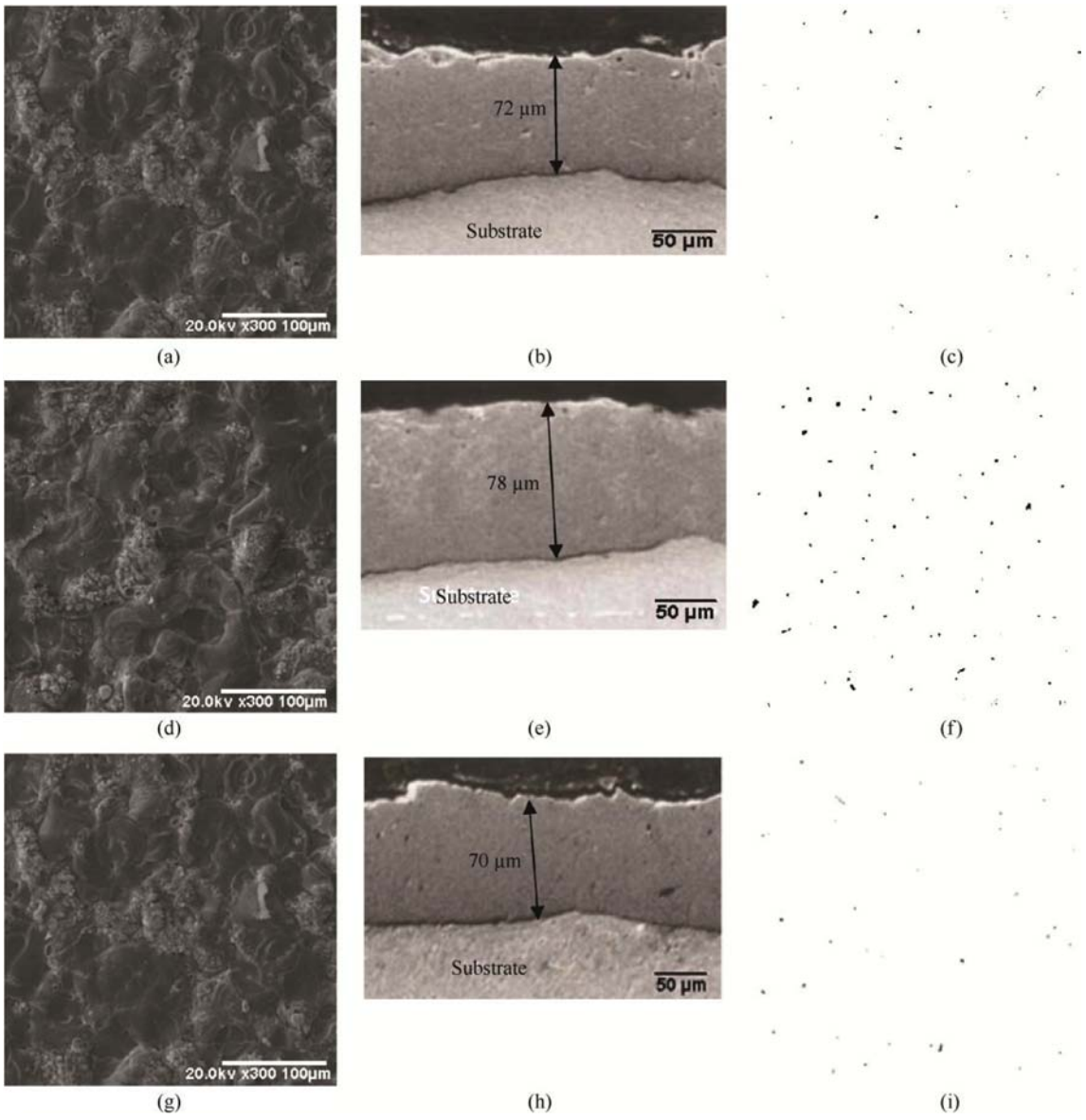

Fig. 5. SEM surface morphology of (a–c) top surface (d–f) cross-section and (g–i) porosity analysis for the minimum (a, d, g), maximum (b, e, h) and optimum conditions (c, f, i).

microscopy (SEM). MAO coat consists of porous coating with a typical discharge channels on the top surface (Fig. 5(a–c)) and the thickness were measured in the cross-section surface (Fig. 5(d–f)). The corresponding porosity of the coating is shown in (Fig. 5(g–i)). For the minimum condition, i.e., lower porosity with higher hardness the coating thickness is to be 72 µm and for the maximum condition, i.e., higher percentage of porosity with lower hardness the coating thickness is to be 78 µm. The MAO parameters are optimised to achieve lower porosity with higher hardness in this the coating thickness is 70 µm.

Fig. 6 illustrates the XRD analysis of the MAO coatings carried out in the optimised condition. In this some aluminium peaks was observed it may be an indication of substrate. A small amount of α-Al_2O_3 present on the top surface layers of the MAO coating and it mainly comprised of γ-Al_2O_3 phase [19].

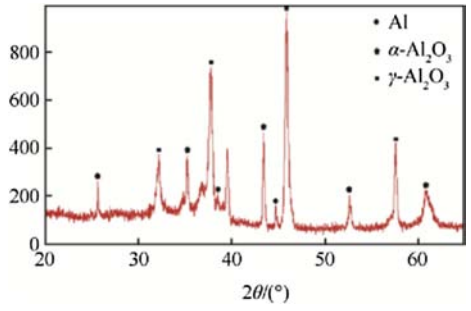

Fig. 6. XRD patterns of MAO coatings deposited at optimised condition.

2. Conclusions

1) Empirical relationships were constructed to determine the porosity and hardness of MAO coatings deposited on the stir

zone of FSW joints of AA6061 aluminium alloy at 95% confidence level, incorporating important MAO parameters.

2) MAO parameters were optimized using response surface methodology to achieve coatings with minimum porosity and maximum hardness. The optimized values (1.76 vol% of porosity and 1360 HV of hardness) are closely matched with the experimentally determined values.
3) Among the three MAO parameters investigated, current density is found to be the predominant factor, followed by oxidation time and inter-electrode distance and this is confirmed by Analysis of Variance test (*F*-ratio).

Acknowledgements

The authors wish to record their heartfelt thanks to Council of Scientific and Industrial Research (G8/19901/2013), New Delhi for the financial support provided to conduct this investigation through sponsored project No. 22(0615)/13/EMR-II dated 26.02.2013.

References

[1] Mishra RS, Ma ZY. Friction stir welding and processing. Mater Sci Eng R Rep 2005;50:1–78. http://dx.doi.org/10.1016/j.mser.2005.07.001.
[2] Su JQ, Nelson TW, Mishra R, Mahoney M. Microstructural investigation of friction stir welded 7050-T651 aluminium. Acta Mater 2003;51:713–29. http://dx.doi.org/10.1016/S1359-6454(02)00449-4.
[3] Threadgill PL, Leonard AJ, Shercliff HR, WJ P. Friction stir welding of aluminium alloys. Int Mater Rev 2009;54:49–93. http://dx.doi.org/10.1179/174328009X411136.
[4] Gholami S, Emadoddin E, Tajally M, Borhani E. Friction stir processing of 7075 Al alloy and subsequent aging treatment. Trans Nonferrous Metals Soc China (English Ed 2015;25:2847–55. http://dx.doi.org/10.1016/S1003-6326(15)63910-3.
[5] Vargel C. Chapter B.6-The corrosion behaviour of aluminium alloys. Corrosion of aluminium. Elsevier; 2004. p. 211–30. http://dx.doi.org/10.1016/B978-008044495-6/50016-1.
[6] Surekha K, Murty BS, Rao KP. Microstructural characterization and corrosion behavior of multipass friction stir processed AA2219 aluminium alloy. Surf Coatings Technol 2008;202:4057–68. http://dx.doi.org/10.1016/j.surfcoat.2008.02.001.
[7] Venkata Rao C, Madhusudhan Reddy G, Srinivasa Rao K. Microstructure and pitting corrosion resistance of AA2219 Al–Cu alloy friction stir welds – effect of tool profile. Def Technol 2015;11:123–31. http://dx.doi.org/10.1016/j.dt.2014.10.003.
[8] Wadeson DA, Zhou X, Thompson GE, Skeldon P, Oosterkamp LD, Scamans G. Corrosion behaviour of friction stir welded AA7108 T79 aluminium alloy. Corros Sci 2006;48:887–97. http://dx.doi.org/10.1016/j.corsci.2005.02.020.
[9] Zaid B, Saidi D, Benzaid A, Hadji S. Effects of pH and chloride concentration on pitting corrosion of AA6061 aluminum alloy. Corros Sci 2008;50:1841–7. http://dx.doi.org/10.1016/j.corsci.2008.03.006.
[10] Gharavi F, Matori KA, Yunus R, Othman NK, Fadaeifard F. Corrosion behavior of Al6061 alloy weldment produced by friction stir welding process. J Mater Res Technol 2014;4:314–22. http://dx.doi.org/10.1016/j.jmrt.2015.01.007.
[11] Rambabu G, Balaji Naik D, Venkata Rao CH, Srinivasa Rao K, Madhusudan Reddy G. Optimization of friction stir welding parameters for improved corrosion resistance of AA2219 aluminum alloy joints. Def Technol 2015;11:330–7. http://dx.doi.org/10.1016/j.dt.2015.05.003.
[12] Jariyaboon M, Davenport AJ, Ambat R, Connolly BJ, Williams SW, Price DA. The effect of welding parameters on the corrosion behaviour of friction stir welded AA2024-T351. Corros Sci 2007;49:877–909. http://dx.doi.org/10.1016/j.corsci.2006.05.038.
[13] Wernick S, Pinner R, Draper R. Surface treatment and finishing of aluminium and its alloys. 1st ed., vols. 1–2. Oxford; New York: Pergamon Books; 1972.
[14] Wernick S, Pinner R, Mason RB. The surface treatment and finishing of aluminium and its alloys. 6. ed., vol. 104. Metals Park, Ohio: ASM International; 1957. http://dx.doi.org/10.1149/1.2428628.
[15] Yang JYF. Surface modification of aluminum alloy products for micro-arc oxidation processes. 2009.
[16] Xiang N, Song R, Zhuang J, Song R, Lu X, Su X. Effects of current density on microstructure and properties of plasma electrolytic oxidation ceramic coatings formed on 6063 aluminum alloy. Trans Nonferrous Metals Soc China 2016;26:806–13. http://dx.doi.org/10.1016/S1003-6326(16)64171-7.
[17] Rama Krishna L, Somaraju KRC, Sundararajan G. The tribological performance of ultra-hard ceramic composite coatings obtained through microarc oxidation. Surf Coatings Technol 2003;163–164:484–90. http://dx.doi.org/10.1016/S0257-8972(02)00646-1.
[18] You Q, Yu H, Wang H, Pan Y, Chen C. Effect of current density on the microstructure and corrosion resistance of microarc oxidized ZK60 magnesium alloy. Biointerphases 2014;9:31009. http://dx.doi.org/10.1116/1.4889734.
[19] Dehnavi V, Liu XY, Luan BL, Shoesmith DW, Rohani S. Phase transformation in plasma electrolytic oxidation coatings on 6061 aluminum alloy. Surf Coatings Technol 2014;251:106–14. http://dx.doi.org/10.1016/j.surfcoat.2014.04.010.